Downhole Seismic Imaging at Les Mines Selbaie

by

David Eaton, Gervais Perron and David Forsyth

October 31, 1996

Contents

1 Introduction

This report provides a summary of results from a downhole seismic imaging (DSI) survey carried out by the Geological Survey of Canada. This project was funded by Les Mines Selbaie through a research agreement tied to a Specified Purpose Account (SPA). The survey was conducted on May 23, 1996 in borehole B1111, located just south of the open pit where active mining for copper and zinc is taking place at Les Mines Selbaie, Quebec (Fig. 1). The objectives of this project are: 1) to investigate the feasibility of DSI techniques for delineating geological contacts in the Selbaie area; 2) to characterize the seismic response of off-hole electromagnetic anomalies observed in borehole B1111; and, 3) to obtain in situ constraints on seismic reflectors observed in the Lithoprobe high-resolution seismic profile 29-2.

Data acquisition and initial processing are described in an earlier progress report (June 19, 1996) and are reiterated here briefly for completeness. This report also describes borehole density and velocity logging from B1111, and compares these results to physical rock properties inferred from borehole B1219 (used primarily to interpret the earlier Lithoprobe survey). Next, this report contains revised processing results for the DSI survey, and concludes with a discussion of seismic modelling and interpretation.

2 Data Acquisition

The data for this survey were acquired in borehole B1111 on May 23, 1996. Although the daytime temperatures at this time of year are well above freezing, it was necessary to clear a thick block of ice in the first few m of the borehole prior to commencing the survey. The collar of the borehole is located approximately 100 m from the edge of the open pit (150 m in depth), where active mining is taking place. The borehole extends in the subsurface beneath the pit, but cable limitations prevented acquisition of data below a wireline depth of 1050 m and the surface projections of all geophone locations are south of the pit. A Bison 6-channel seismic recorder connected to a PC-AT laptop computer was used to record the seismic signal. Only 4 of the 6 channels were used, for 1 surface channel (a geophone placed in the ground near the recorder) and 3 downhole channels. The downhole seismic tool consisted of a Geosource sonde, housing three 14 Hz geophones mounted such that one geophone (V, for vertical) records the component of wave particle motion that is directed along the axis of the borehole, and the other two geophones (H1 and H2, for horizontal) record mutually orthogonal components of particle motion in the plane perpendicu-

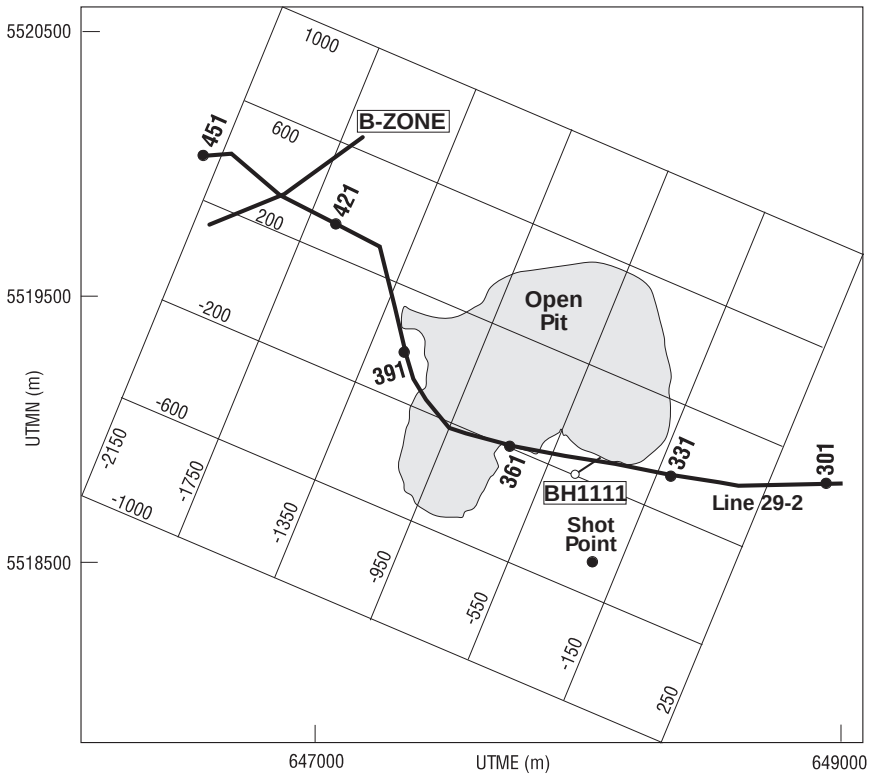

Figure 1: Location map of the DSI survey in borehole B1111, also showing the location of the Lithoprobe high-resolution line 29-2.

lar to the borehole axis (Fig. 2). The sonde is held fixed to the wall of the borehole using a clamping arm. A total of 175 shots were recorded approximately every 5 m, between 1061 and 183 m depth.

The seismic source consisted of one (or two) 227 g pentolite boosters detonated using 0-msec blasting caps. In order to reduce costs for this survey, an existing body of water (a settling pond located south of the open pit) was used to fire the shots. The shooting location was situated at a sampling marker (D4A) at barrier built of mine aggregate material between two segments of the settling system. The charge was suspended in 2-3 m of water. The initial 59 shots, corresponding to the deepest receiver levels, were fired using 2 boosters. The remaining shots were fired with a single booster. Once started at 11:00 am, data acquisition took 8.5 hours to complete.

Accurate timing of the shots was achieved using shooting boxes owned by the GSC, which have very accurate internal clocks that trigger on every minute mark. Two boxes were used, one at the recorder to trigger the Bison recording system, and one at the shooting location.

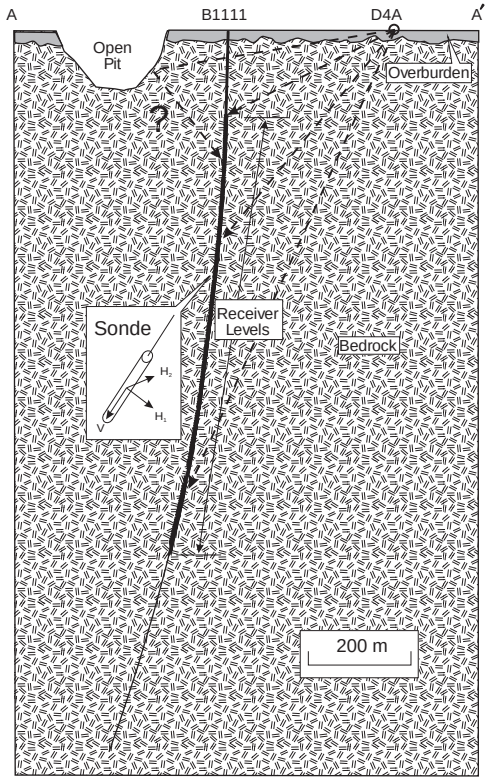

Figure 2: Cross section of B1111. Dashed lines with arrows show raypaths for direct arrivals from the shot and a reflection from the open pit (marked ?).

3 Borehole Logging Data

As part of a separate project, density and full-waveform sonic logs (Fig. 3) were acquired in borehole B-1111 by the Mineral Resource Division (MRD) of the GSC. In situ density values were measured using a gamma-gamma tool with a 10 cm sampling. The P-wave velocity at each depth sample was determined using the compressional

first arrival traveltimes. In addition, the acoustic impedance was computed using the product of density and P-wave velocity. Note that the logs shown in Fig. 3 have been resampled to every meter using a running average of 10 samples. Thin black lines on each log plot show the median data value within each individual lithologic unit.

A lithological log for B1111 was also provided by Les Mines Selbaie. The main lithological units encountered in B1111 were: 1) Welded Acid Tuff (WAT), 2) Dacite Tuff (DT), 3) Andesite Tuff (AT), 4) Rhyolite (R), 5) Felsic Dykes (FD) and 6) Massive Sulphides (MS).

Finally, Fig. 3 also shows the corresponding synthetic seismic trace for the density and velocity logs. The synthetic trace was constructed in the frequency domain by multiplying the reflection coefficient function with a Ricker wavelet with a central frequency of 50 Hz. By comparing the synthetic seismogram with the lithology log, we can conclude that most of the reflectivity in the vicinity of borehole B1111 is caused by lithological contacts (prominent reflections will arise from the contact between two lithologies with a large impedance contrast). This is in agreement with results presented by Perron *et al.* (submitted) using logs from another deep exploration borehole in the Selbaie mining camp (B1219).

The median values for density and P-wave velocity for each lithology are presented in Fig. 4. Ellipses represent the distribution of 1 standard deviation of the samples around their median values. Plotted in the background are the acoustic impedance contour lines. As described by Salisbury *et al.* (1996), massive sulphides (130-158m) show the largest impedance values (32). These large values are the result of unusually high density and velocities readings. Aside from the massive sulphides, the FD (508-520m) is the lithologic unit with the highest mean velocity (6.2 km/s), leading to a characteristic high impedance value (24). The family of tuffs (WAT, DT and AT) have values ranging from 2.55 to 2.85 g/cm3 (density) and from 5.6 to 6.1 km/s (P-wave velocity). Increasing velocity and density is in positive correlation with the percentage of mafic minerals in each tuff unit. The WAT is the most felsic tuff and shows characteristics similar to rhyolites, while the AT is the most mafic. Values associated with DT lie in between the two end members of the family. Variations within a single tuff type seem to be associated the presence of lapillis, yeilding to increased values in density.

Figures 5 and 6 show the results for borehole B1219 after the same data analysis. B-1219 begins in the Brouillan Tonalite (T), intersects the faulted contact between the tonalite and the Selbaie Andesite (A) and runs through more than 900 m of Rhyolite/Welded Acid Tuff (R) and Dacite Tuff (DT) sometimes intruded by Felsic Dykes (FD). It is important to note that the data for B1219 was collected by Atomic Energy of Canada Limited (AECL) and that there is a difference in calibration between

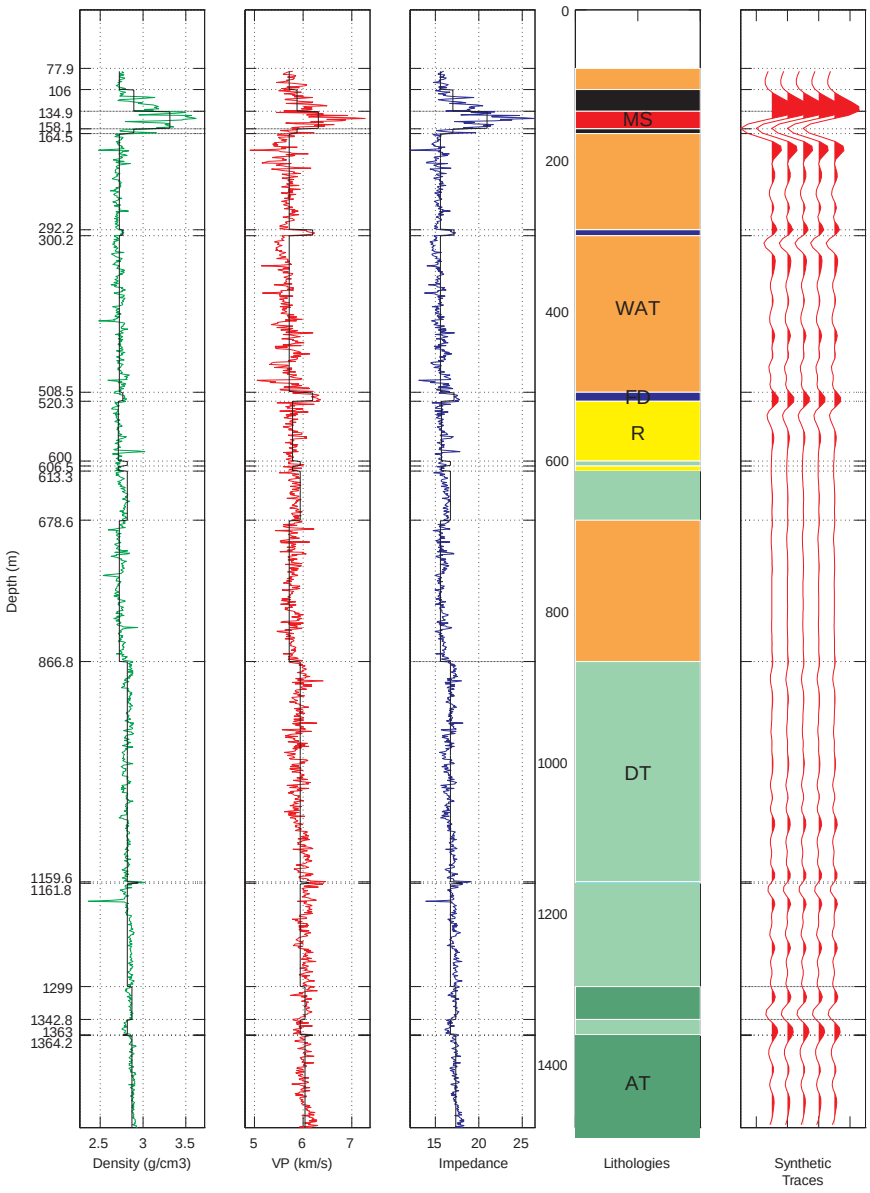

Figure 3: Borehole B1111 lithological and geophysical information.

their gamma-gamma tool and the one from MRD. This can account for part of the mismatch between values for the same lithology acquired in two different boreholes.

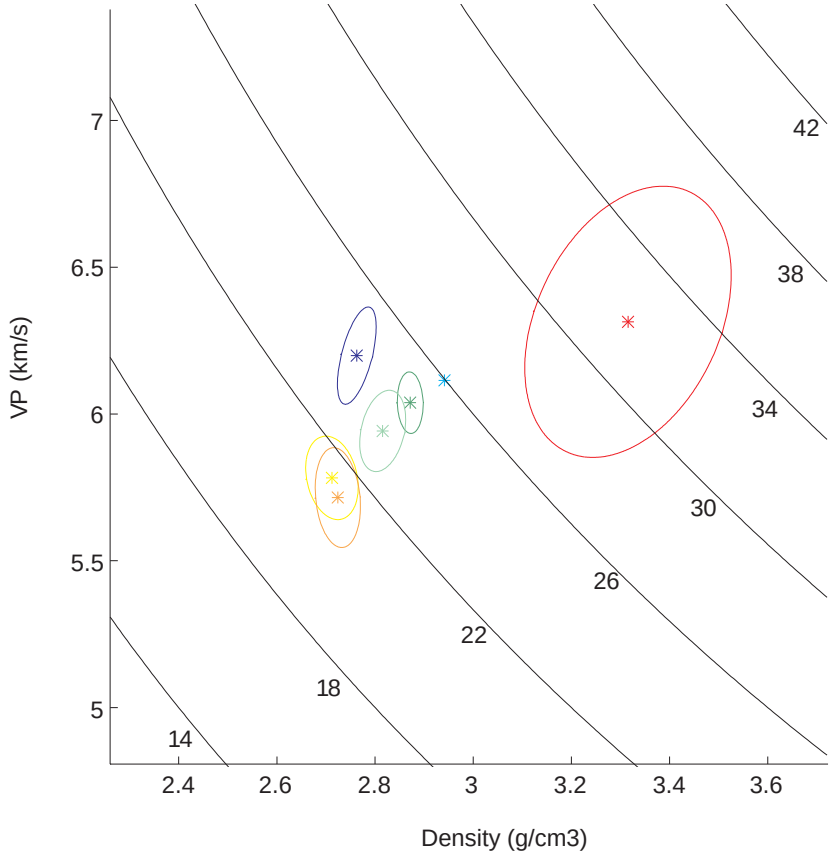

Figure 4: Crossplot diagram of the physical rock properties for each lithology encountered in borehole B1111

In B1219, WAT and Rhyolites were grouped together (under Rhyolite). They still show the lowest densities, but the mean velocity value is increased. Those anomalously high values correspond to a pyrite mineralization (475-720m). Low values for tonalite and andesite are related to the fractured nature of the upper part of the bedrock. Values obtained for DT and FD are in agreement with those observed in borehole B-1111.

4 Revised Processing

The initial processing of the Selbaie DSI data is described in the progress report of June 16th, 1996. The processing sequence has been revised and now incorporates a broader frequency range, F-K dip filtering and energy balancing.

The first important step in processing DSI data is to rotate the horizontal components in such a way that one of the component points towards the shot location (radial component). The other horizontal component will therefore point in a direction perpendicular to the shot location (transverse component). This is done in order to compensate the rotation of the DSI tool as it moves up and down in the borehole. One consequence of the rotation is the maximization of the P-wave response on the radial component and the S-wave response on the transverse component.

The different types of signal in a DSI section can be classified as "downgoing", which includes direct P and S-wave arrivals (and some scattered energy, as in Fig. 7), and "upgoing", which represents reflected and/or scattered energy. The upgoing waves are much weaker than the downgoing waves and are not visible in a spectral balanced section (Fig. 7). Filtering of the downgoing arrivals is achieved by applying a median filter to the P-wave arrivals for the radial and vertical components and on S-wave arrivals for the transverse component. This procedure efficiently removes all signals with dips equal to the P and S-wave first arrivals, respectively.

To remove other downgoing signal, such as tube waves, a frequency-domain dip filter is used. On a frequency-domain plot (frequency vs. wavenumber) the downgoing signal corresponds to positive wavenumbers while the upgoing signal has negative corresponding wavenumbers. By substracting the contribution of all positive wavenumbers the remaining signal contains only reflected energy and random noise.

Finally, the filtered traces are energy balanced to improved the continuity of the reflections. This procedure consists of a gain control with single-window energy equalization. For each trace in the section, the energy is computed in a single time window and the entire trace is multiplied by a factor proportional to the inverse of the square of the amplitude.

Table 1 presents in details the parameters used for each processing steps. Results from the reprocessing of the Selbaie DSI data are shown in Figs. 8-10.

Table 1. Processing Sequence

1)	Shot depth statics	
2)	Rotation of the components	energy maximization, 25 ms window centered on P-wave first arrivals
3)	Spectral Balancing	35 to 225Hz, 10Hz window, 500ms AGC
4)	Top Mute	amplitude set to 0 from 0 sec to P-wave first arrival
5)	Median filtering	13 traces
6)	F-K filtering	all positive wavenumbers muted
7)	Energy balancing	0.5 sec window

5 Modelling

In order to determine the seismic expression of various geological and morphological features, a seismic forward modelling study has been conducted. The seismic modelling makes use of 3-D seismic modelling software developed at the GSC (Eaton, 1996). The modelling software allows the source-receiver geometry to be duplicated exactly. Three key features have been examined using this approach: 1) the B-zone (Fig. 1), a fault-controlled zone of chalcopyrite and sphalerite mineralization that dips at approximately 45 degrees to the southeast (Perron et al., 1996); 2) the open pit, assumed to be vertically sided and 100-m deep; and, 3) a hypothetical localized scattering anomaly, located at a depth of 607 m, and situated 100 m west of the borehole. For the purpose of generating a seismic modelling result, the B zone is assumed to continue with no change in dip to a depth of 2 km.

The modelled seismograms are shown in Fig. 11. The data were generated using a centre frequency of 80 Hz, and a background velocity of 5.8 km/s. The three components are oriented in the UTM reference frame (easting, northing and vertical). In an approximate sense, these components correspond, respectively, to the transverse, radial and vertical components. This modelling study includes P waves, S waves and mode-converted waves (P-S and S-P). A number of observations are possible from the modelled data: 1) any reflection from the B zone will occur late in the section, although the exact arrival time is dependent on the assumption of constant dip and the seismic velocity used; 2) diffracted arrivals from the hypothetical scattering body will have a characteristic curvature that should be relatively easy to recognize in the section (note that all possible scattering modes have been included in the modelling); 3) the reflections from the pit are "ringy", since arrivals from different parts of the pit will arive at different times. Note that some arrivals appear more prominently

on one component than others. For example, the reflection from the B zone is most prominent on the UTME traces.

6 Interpretation

The borehole logging results show that good reflections are expected from the felsic dykes. This is most easily seen in the reprocessed vertical component section (Fig. 8), where a conspicuous upgoing reflection is visible between 0.13 s and 0.15 s. This reflection originates from the felsic dyke at 508 m in the borehole. Aside from this reflection, the vertical and radial component sections show very weak reflectivity. This is generally consistent with the borehole logging results for B1111, which indicate relatively little variation in velocity and density, with the exception of felsic dykes and massive sulphides.

Some of the arrivals on the transverse component (Fig. 10) are more interesting. This component is more sensitive to P-wave reflections from east-dipping interfaces than are the other two components, as indicated by the synthetic modelling. A fairly continuous refleciton is visible between 300-900 m depth at 0.29 - 0.31 s. This signal arrives earlier than the predicted time for the B zone (or its associated fault zone), but could possibly be related to the B zone if the dip flattens with depth rather than remaining uniform as assumed in the model. A fairly prominent curved arrival is visible at 450 - 600 m depth between 0.16 - 0.2 s. We speculate that this event might be a diffraction from a localized scattering body, since it matches fairly well the event PSs shown in Fig. 11. Note that the downward-propagating scattered arrival corresponding to this feature is visible in the spectral balanced record section for the transverse component (arrow in Fig. 7). This feature does not appear to correlate with any of the offhole EM anomalies identified in B1111, although it is relatively close to the upper part of the largest anomaly at 700 m depth.

The P-P reflection from the B zone has also been modelled for the shot-receiver geometry corresponding to line 29-2. The modelled data are compared with the observed seismic profile in Fig. 11. Note that the modelled arrival time for the B zone comes after the observed reflection III. This discrepency does not necessary imply that reflection III is from a different feature; instead, it may mean that the B zone (or its associated fault) flattens with depth. This interpretation is consistent with the interpretation of the transverse-component DSI data.

Borehole B1111 extends as far down as zone III in the reflection profile, although no reflective feature was encountered in the borehole. It should be noted that the unmigrated version of the seismic profile is shown here, so the true location of the

dipping reflector is shifted to the east of its apparent position in the profile.

Reflection zone II in the profile intersects the borehole trace at approximately the correct depth for the 508 m felsic dyke. Since this feature produces such a good reflection in the DSI survey (Fig. 8), it seems reasonable to attribute reflection II to the felsic dyke.

7 Conclusions

A DSI survey was conducted in borehole B1111 to characterize the reflectivity of adjacent rock units, with emphasis on the seismic characterization of offhole EM anomalies.

Borehole logging results from B1111 indicate a relative lack of reflective contacts, with the exception of felsic dykes and massive sulphides (which are too shallow to be detected by the DSI method). Similarities in terms of physical rock properties for each lithology between boreholes B1111 and B1219 can be observed. Slight differences between the datasets can be explained in terms of mineralization, presence of lapillis and fractures (or faults) in the first 200 m of the holes, and the use of different acquisition equipment in each case.

Reprocessing of the DSI data, with emphasis on achieving the widest frequency bandwidth possible and removal of downgoing waves with minimum contamination by artifacts, has indicated several interesting reflections. The vertical component record indicates a strong reflection from a felsic dyke at 508 m, as expected. The transverse component record shows reflections that may be coming from west of the borehole. A continuous event that arrives well after the direct arrivals may be associate with the B-zone or related fault(s). If this interpretation is correct, its occurence before the modelled arrival time implies flattening with depth. A scattering anomaly is apparent in the transverse-component data, both before and after removal of the direct arrival (Figs. 7 and 10). This event can be modelled as a P-S diffraction from a localized scattering body at a depth of 607 m, situated 100 m west of B1111. This location is just above a large offhole EM anomaly.

Comparison of the modelling results with the Lithoprobe profile 29-2 indicates that reflection zone III of Perron et al. (1996) may be related to the B zone. We interpret reflection zone II as a felsic dyke intersected by B1111.

8 References

Eaton, D.W. 1996. BMOD3D: A Program for Three-Dimensional Seismic Modelling Using the Born Approximation. GSC Open File 3357.

Perron, G., Milkereit, B., Reed, L., Salisbury, M., Adam, E. and Wu, J. 1996. Integrated seismic refleciton and borehole geophysical studies at les Mines Selbaie, Quebec. Submitted to CIM Bulletin.

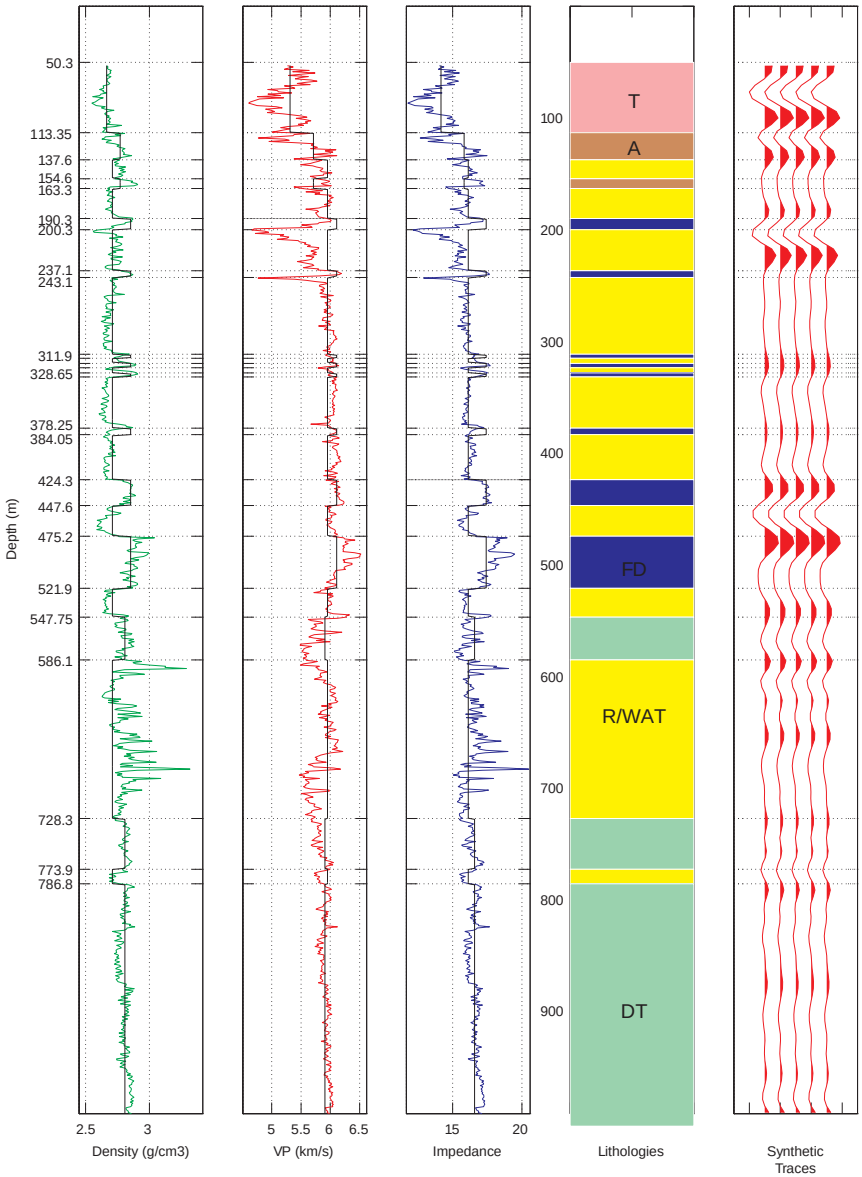

Figure 5: Borehole B-1219 lithological and geophysical informations.

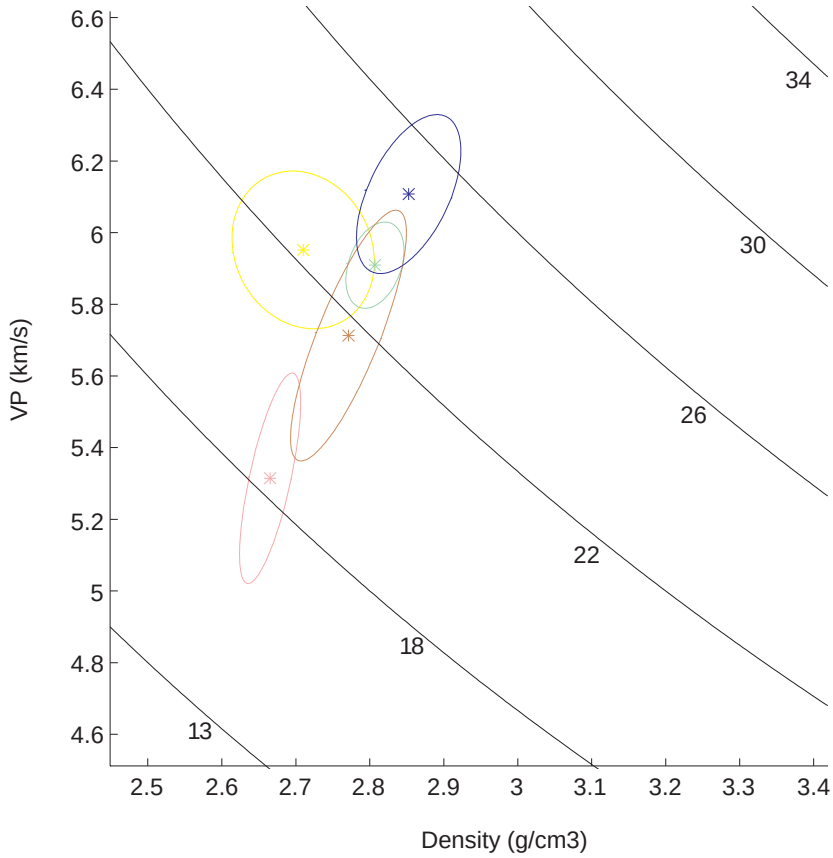

Figure 6: Crossplot diagram of the physical rock properties for each lithology encountered in borehole B-1219

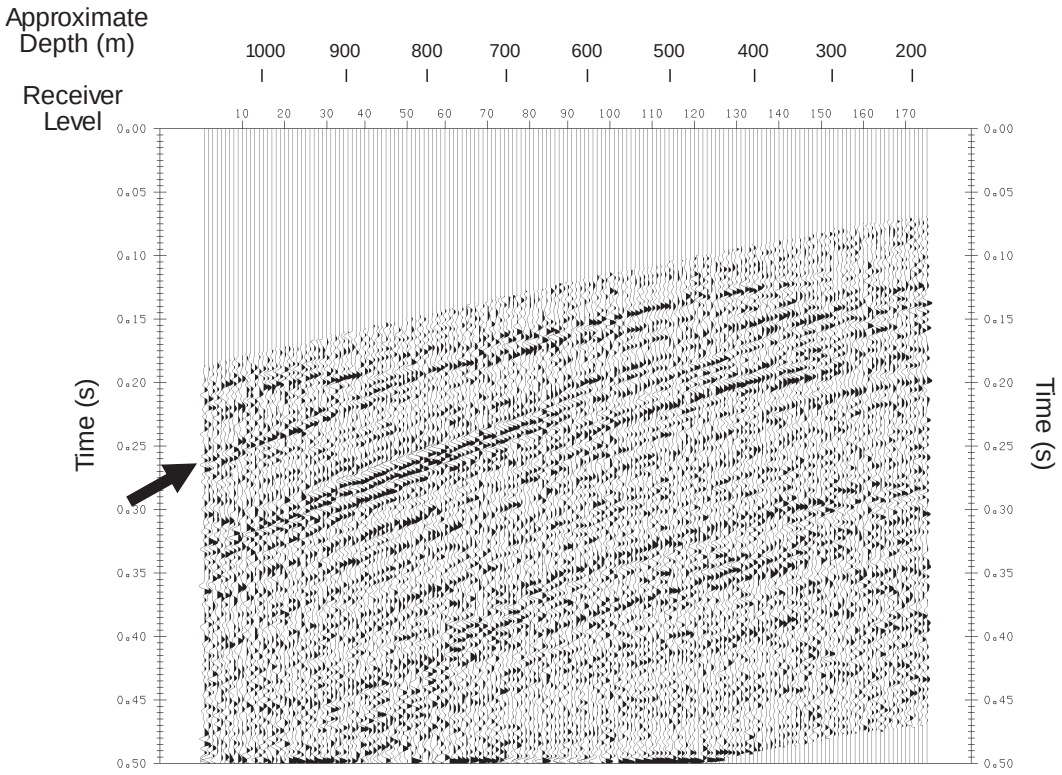

Figure 7: Transverse component record with spectral balance applied, but no removal of downgoing components. Arrow shows a downgoing mode-converted arrival. Comparison with modelling results suggests that this may be related to a scattering body at 600 m depth.

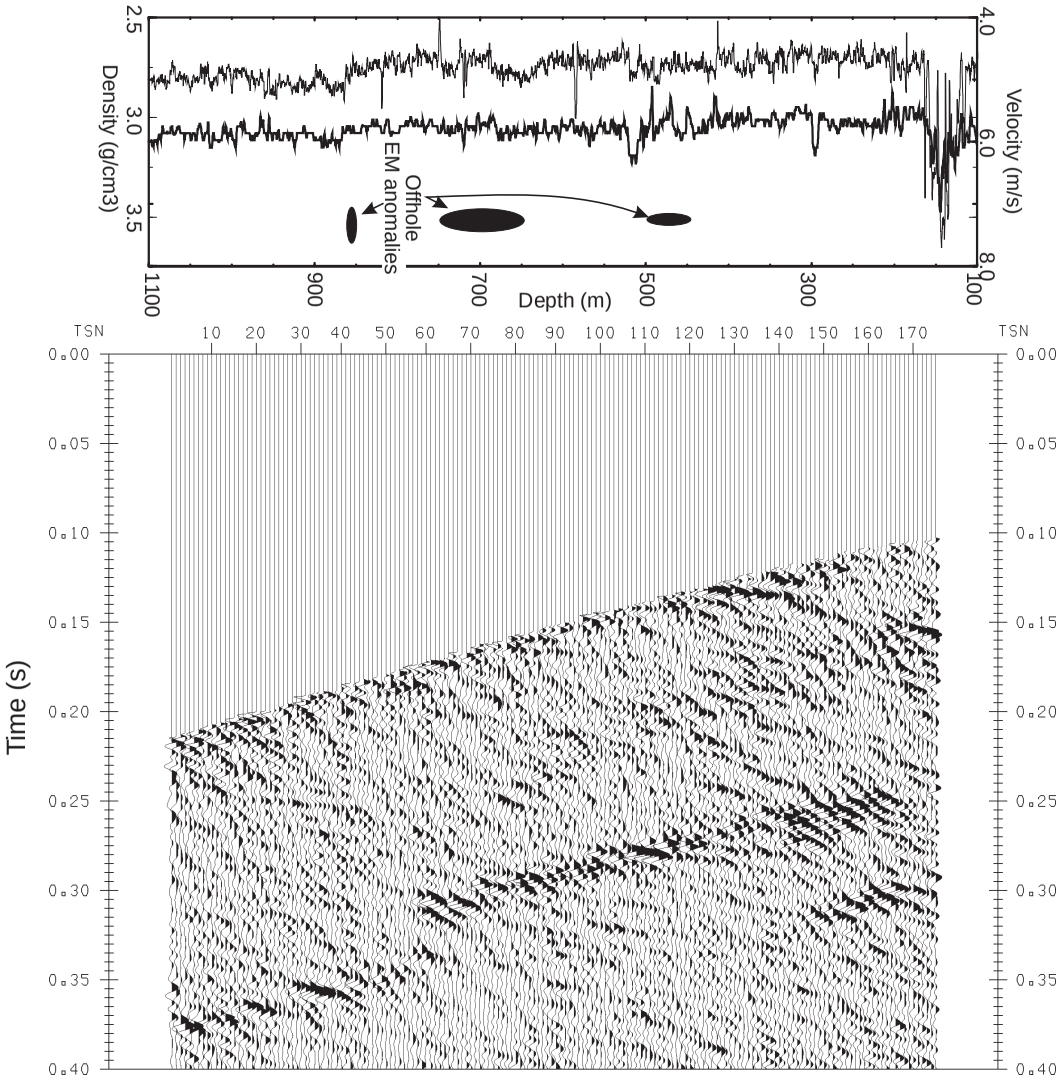

Figure 8: Reprocessed Vertical component

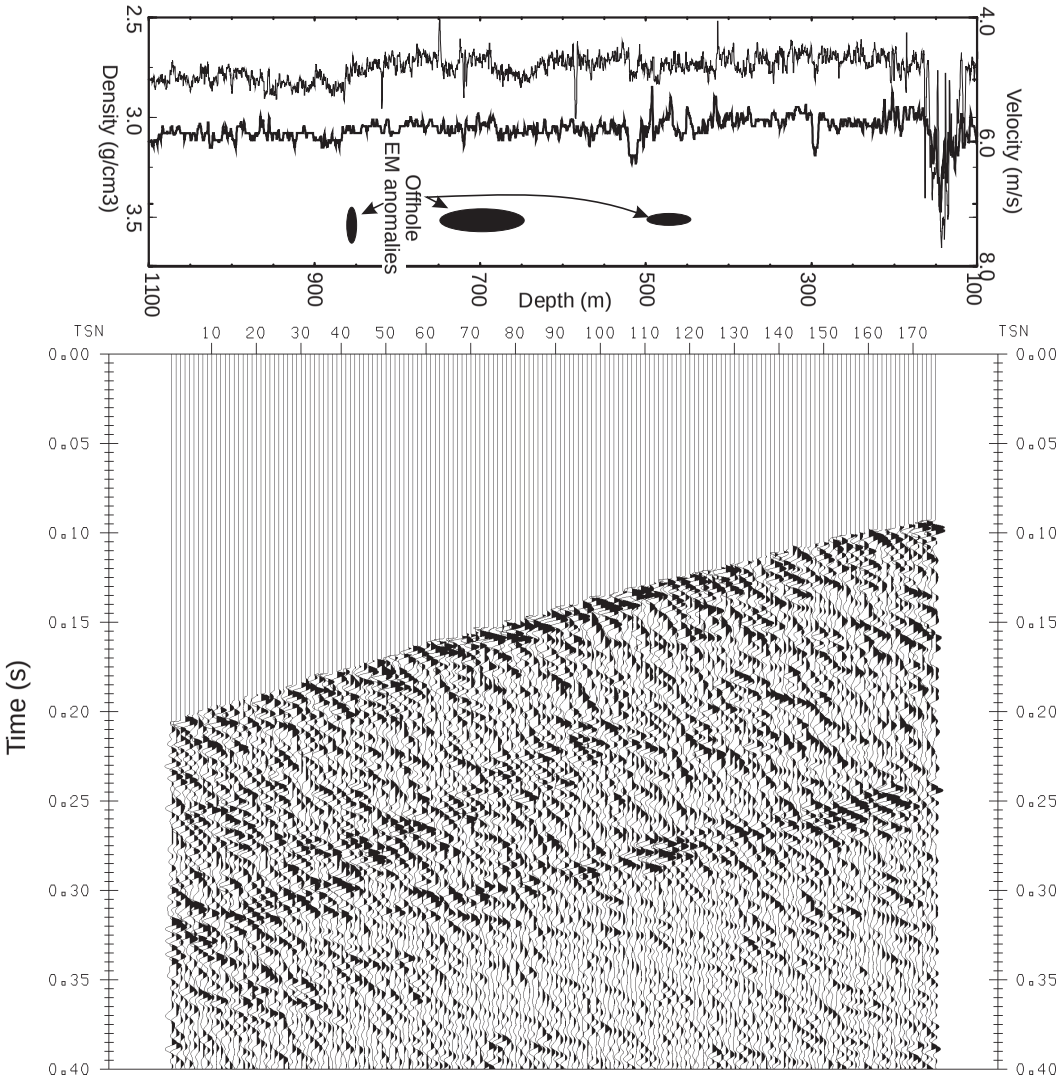

Figure 9: Reprocessed Radial component

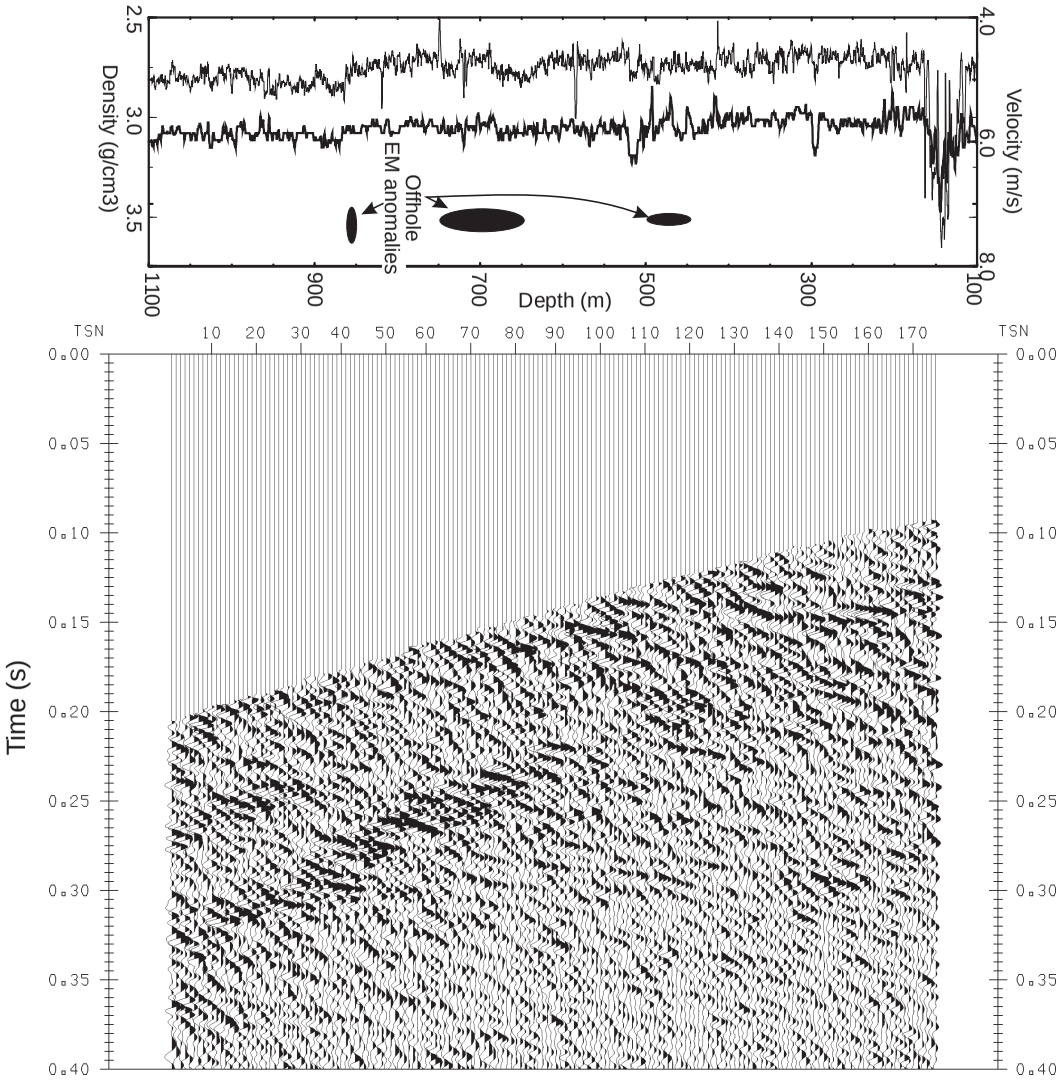

Figure 10: Reprocessed Transverse component

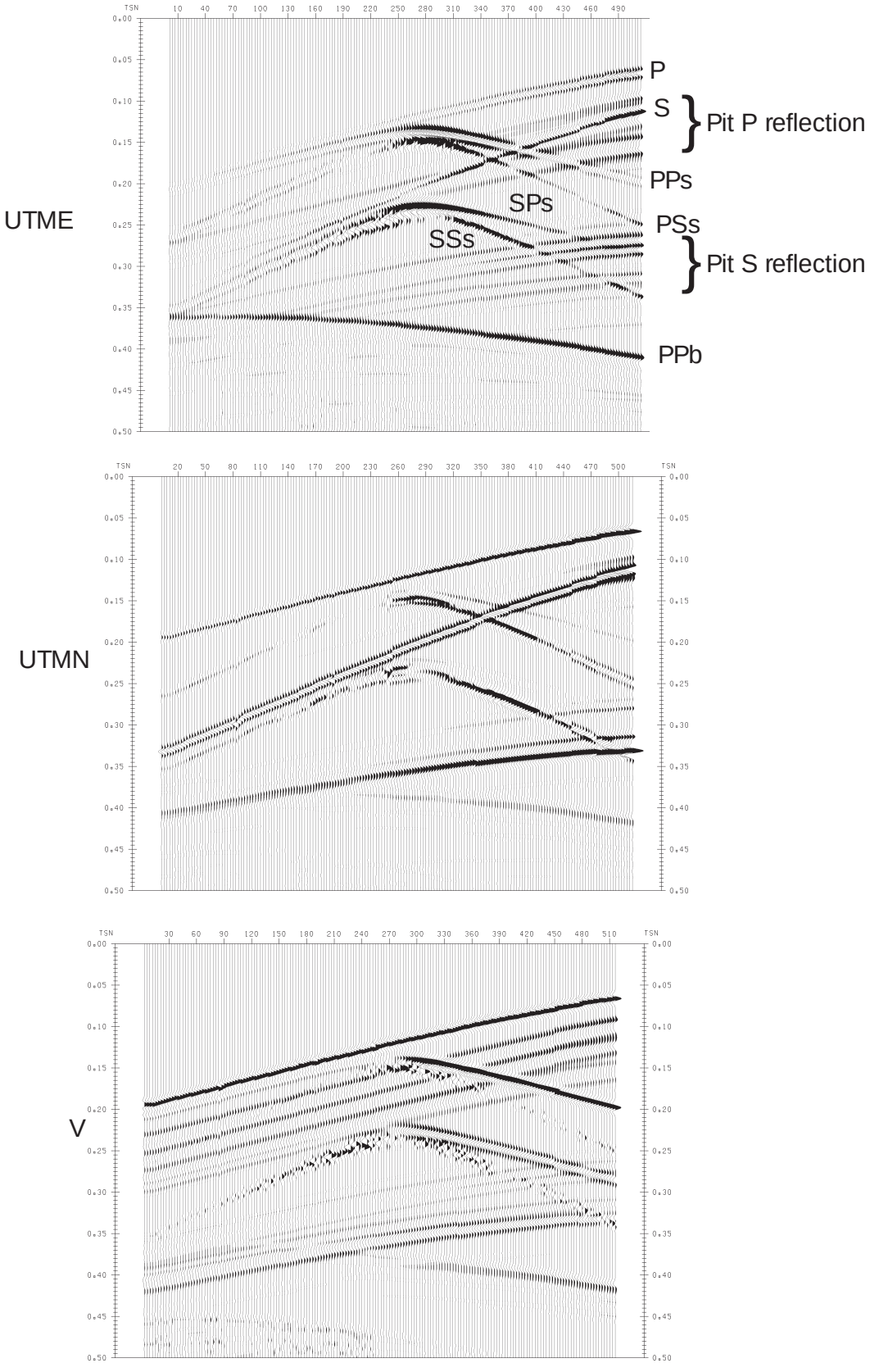

Figure 11: Modelled seismogram. Scattered events have been labelled in the UTME

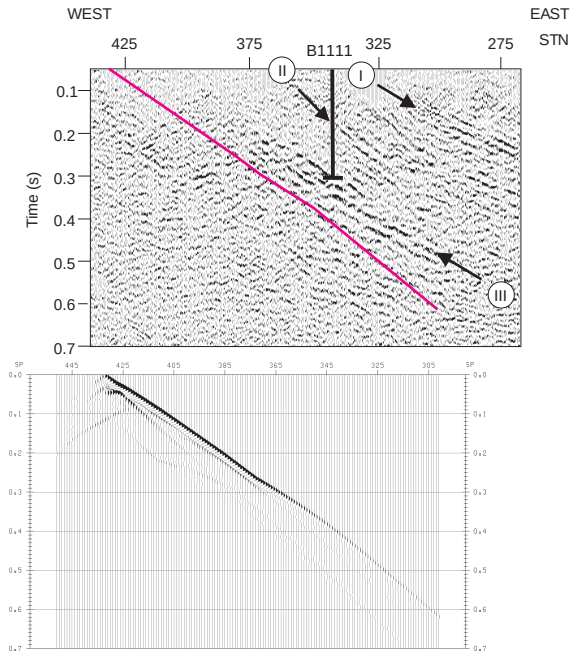

Figure 12: Comparison of the modelled reflection from the B zone (below) with the unmigrated data from Lithoprobe line 29-2 (from Perron et al., 1996). The modelled reflection arrives later than the observed event III. This discrepency could be explained if the B zone flattens with depth.

;